

## Fatigue testing of the fir tree root of a turbine blade

Petr Měšťánek,<sup>1</sup> Zdeněk Kubín<sup>2</sup>

**Abstract:** The present paper deals with the low cycle fatigue of a low pressure steam turbine blade. Nonlinear FEA modeling is used to determine the strain and stress distribution. The lifetime is predicted employing LPSA method in conjunction with uniaxial fatigue criterion SWT. Experimental testing procedure to verify the FEA analysis and lifetime prediction is described. Strains measured employing strain gauge measurement are compared to numerically calculated strains. Predicted lifetime is compared to experimentally determined lifetime and the reasons of differences are discussed.

**Keywords:** Low cycle fatigue, Experimental fatigue testing, Strain gauge

### 1. Introduction

The demand for high-efficiency steam turbines is increasing due to increasing cost of electricity and environmental issues. The most promising way how to reduce the exhaust loss and increase efficiency of the steam turbine is to extend the end low pressure blade. However, the longer the airfoil of the blade is the more severely loaded is the blade-disc connection due to centrifugal forces. Particularly, in the case of non-shrouded blades the airfoil must be massive enough to avoid problems in dynamic behavior. As a result, the centrifugal forces cause extreme loading of the blade root that is typically equipped with the fir-tree type of root. Usually, the blade material goes locally plastic at the operational speed of 3000-rpm.

As the whole turbine is repeatedly started up and shut down, the varying centrifugal force results in repeated plastic strain inside the blade material. This can lead to crack initiation and consequential low cycle fatigue (LCF) failure of the whole blade. Therefore, low cycle fatigue of the low pressure steam turbine blades must be taken into consideration.

The current paper deals with the experimental testing of the fir-tree root. This testing is aimed at the verification of the computational prediction of the low cycle fatigue lifetime. First, the number of cycles to fatigue crack initiation at a low pressure blade is predicted using FEA simulation and uniaxial fatigue criteria. In order to verify the prediction, scaled model of the fir-tree root was designed and cyclically strained. The objective of the fatigue testing was to measure strain

---

<sup>1</sup> Ing. Petr Měšťánek; University of West Bohemia; Univerzitní 8, 30614 Plzeň, Czech Republic; mestanek@kme.zcu.cz

<sup>2</sup> Ing. Zdeněk Kubín; Škoda Power a.s. A Doosan Company; Tylova 1/57, 30128 Plzeň, Czech Republic; zdenek.kubin@doosanskoda.com

distribution using strain gauges; to localize the crack initiation; to monitor the initiation phase of the fatigue crack and to obtain number of loading cycles to fatigue crack initiation. These outcomes were intended to be compared to that predicted computationally.

## 2. Low pressure turbine blade – computational lifetime prediction

Local Plastic Stress and Strain Analysis (LPSA) approach was used to predict number of loading cycles to fatigue crack initiation [1]. One loading cycle corresponds to one start up (3000 rpm) and shutdown of the turbine. In addition, there are atypical loading cycles in the loading spectrum of the turbine: one balancing cell over-speed test (typically 3600 rpm) and app. 40 over-speed tests (typically 3300 rpm). However, these cycles are not included in the prediction and are discussed later.

Stress and strain distribution at the blade root was determined using nonlinear contact elastic-plastic FEA analysis. Multilinear kinematic hardening material model was used for both rotor and blading material. Cyclic strain curve for both materials was examined experimentally using simple specimens. Equivalent strain distribution from concave side of the root is depicted in Fig. 1a) for loading and in Fig. 1b) for unloading. Figure 1b) represents the residual strain.

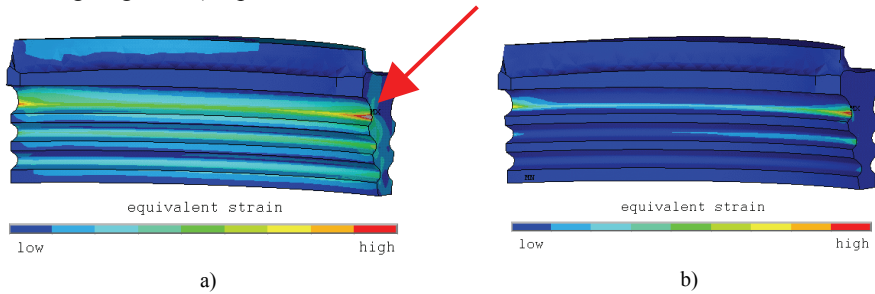


**Fig. 1.** Equivalent strain distribution at the blade root (from concave side) a)loading; b) unloading - residual strain.

Local Plastic Stress and Strain Analysis (LPSA) approach was selected for fatigue assessment. The real elastic-plastic state of stress and strain at the critical node is the fundamental input into LPSA method. Stress and strain components are calculated using nonlinear FEA simulation. Reduction of the triaxial state of stress and strain is carried out employing von Mises rule [2]. Amplitude of equivalent stress and strain is calculated as described in [1]. Uniaxial Smith, Topper, Wetzel (SWT) damage parameter ( $P_{SWT}$ ) was used to determine the number of cycles to fatigue crack initiation:

$$P_{SWT} = \sqrt{(\sigma_a + \sigma_m) \varepsilon_a E} = \left[ \sigma_f'^2 (2N_i)^{2b} + E \sigma_f' \varepsilon_f' (2N_i)^{b+c} \right]^{0.5}, \quad (1)$$

where  $\sigma_f'$ ,  $b$ ,  $\varepsilon_f'$ ,  $c$  are parameters defining the Manson-Coffin curve of the material,  $E$  is the Young's modulus,  $\sigma_a$  is the stress amplitude,  $\sigma_m$  is the mean stress,  $\varepsilon_a$  is the strain amplitude and  $N$  is the unknown number of cycles to crack initiation

The location of the first fatigue crack initiation was predicted at the first groove of the fir-tree root at the convex side below the inlet edge of the airfoil.

### 3. Specimen design

Above described lifetime prediction is based on low cycle fatigue testing of simple normalized specimens. To verify the prediction itself some specimen that incorporate factors of notch, strain gradient, size etc. must be designed.

Endo, Kondo and Kadoya designed [3] full-scale testing of the whole blade employing four hydraulic cylinders. Nevertheless, this approach requires special testing apparatus and a fatigue testing machine capable of educing thousands of kN.

Hence, it was decided to develop unique scaled specimen. The chosen proportional scale factor was 0.56:1 to the original blade root. This scale factor was chosen with regard to the technological reasons and the testing machine that was available. The specimen (see Fig. 2) comprises of two opposite-orientated fir-tree roots. Bottom fir-tree root (depicted in white) is the exact geometrical model of the real fir-tree root. Top dovetail (depicted in gray) is intended to transmit loading from the testing machine into the bottom dovetail.

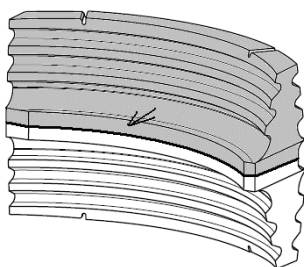


**Fig. 2.** Testing specimen.

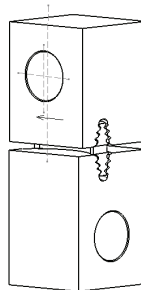


**Fig. 3.** Testing assembly: testing specimen inserted into the fixing jaws.

The transmitted loading must be analogical to centrifugal loading caused by the airfoil. In order to compensate centrifugal loading of the airfoil, top dovetail is shifted towards the concave side of the fir-tree root. This introduces additional bending moment into the specimen. This bending moment is analogical to the moment caused by the misalignment of the radial line of the airfoil and the plane of minimal moment of inertia of the fir-tree root in the case of the real blade.

The specimen is inserted into grooves in fixing jaws (see Fig. 3). The force from testing machine is transmitted to the jaws by pins inserted into holes. In order to accomplish same strain and stress distribution in the model and in the blade, hole in the upper jaw is shifted as illustrated in fig. 3. The optimization of the whole testing assembly was performed using FEA and the same stress and strain distribution in the bottom fir-tree root as in the real blade root was achieved.

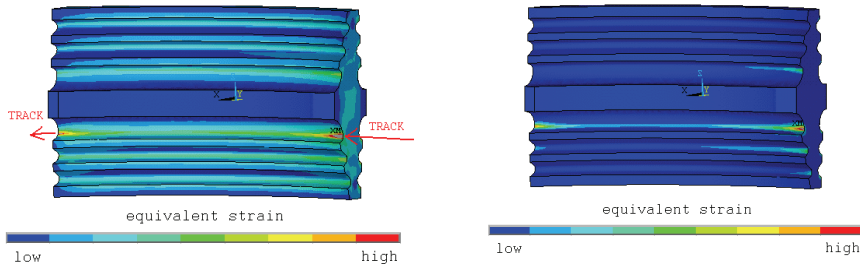


**Fig. 4.** Equivalent strain distribution at the specimen (from concave side) a) loading; b) unloading - residual strain.

Equivalent strain distribution from concave side of the root of the testing specimen is depicted in Fig. 4a) for loading and in Fig. 4b) for unloading. Figure 4b) represents the residual strain. Figure 5 shows comparison of total equivalent strain and plastic strain intensity distribution of the real blade and testing specimen along the track depicted in figure 4a).

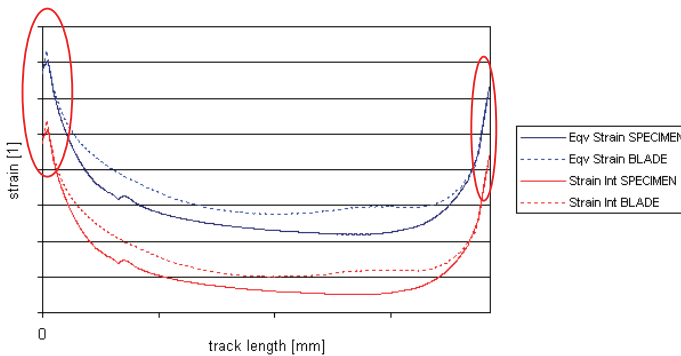


**Fig. 5.** Comparison of total equivalent strain and plastic strain intensity distribution of the real blade and testing specimen along the track depicted in figure 4a)

Since the testing specimen is scaled, several conditions must be met. Gradients and also absolute values of equivalent strain and strain intensity for testing specimen and for blade are same in the designated areas (the locations of expected fatigue crack initiation). Stress distribution is equivalent as well. Therefore, the scale factors for stresses and strains equal one. The testing specimen is made of blading material; hence, the scale factor for all material properties equals one as well. All dimensions of the specimen are scaled by the scale factor 0.56. External forces and the position of the top dovetail are optimized so that the strain and stress distribution in the specimen is analogical to that in real blade.

Since all similarity conditions have been met the testing specimen and the fir-tree root of the LP blade are similar [4]. Hence, number of cycles to fatigue crack initiation of the blade and of the test specimen equal.

## 4. Experimental testing

### 4.1. Testing specimen

The testing specimen was manufactured employing the same technology as in the case of the real fir-tree root. Numerically controlled mill equipped with the custom made cutter head was used to machine the specimen. Same procedure was used when machining the groove in the fixing jaws. Fixing jaws were finished using standard machine tools. The specimen is made of blading material (pole timber) and the fixing jaws are made of rotor material (forging) like the blade-rotor couple.

All transverse profiles of the fir-tree specimen were measured using 3D contour measuring system ZEISS. All dimensions were in accordance with the design tolerances. However, all deviations from the nominal dimensions were recorded in order to be able to retroactively evaluate the influence of manufacturing inaccuracies on the fatigue behavior

Test assemblies are assembled using standard procedures for blading assembly. The specimen was fixed in the fixing jaws using wedges. Five testing assemblies were prepared. The force from the testing machine is transmitted into testing assemblies through pins inserted into holes drilled into jaws. The holes are rectangular to each other (see Fig. 3) to avoid problems concerning inaccuracies of the manufacturing, assembly and the imperfections of the testing machine.

### 4.2. Strain gauge measurement

Foil strain gauges from HBM type 1,5/350LY11 were used for static measurement. The strain gauges were attached by special glue EP 310 S (from HBM) developed for high temperatures and extreme strains. The glue is hot curing two component epoxy resin adhesive which provided good service during residual stress measurement.

First the groove casts were made of Lukopren N which is two-component silicon rubber. Then the strain gauges were tacked by an adhesive tape. The positions of strain gauges were fixed, the glue was added and the silicon rubber cast was placed. Glued strain gauges were cured under pressure at the temperature of 280°C for 4 hours.

Amplification of the signals from strain gauges was carried out by 8<sup>th</sup> balanced ¼ bridge power amplifiers from HIO Jelen Company, Prague. Initially, signal levels from the strain gages were in  $\mu\text{V}$  and subsequently in mV after the amplification. The bridges can amplify direct (0 – 3Hz) or alternate (3 – 1000Hz) signal or both together. Just the direct amplification was used with nominal amplification  $A_{\text{DC}} = 100$ . The relation between measured voltage and strain is defined by equation (2):

$$U_M = \frac{1}{4} \cdot A_{DC} \cdot k \cdot \varepsilon \cdot U_F = \frac{1}{4} \cdot A_{DC} \cdot \frac{\Delta R}{R_T} \cdot U_F, \quad (2)$$

where  $U_M$  is the voltage measured,  $U_F = 5V$  is the supply voltage,  $k = 2$  is the strain gauge sensitivity and  $R_T = 350\Omega$  is the nominal resistance of the strain gauge. The “electric” calibrations of all measuring chains (gauges, wires, amplifiers) were performed adding parallel resistance of 100 k $\Omega$ . Then, measuring the voltage  $U_M$ ,  $\Delta R$  and computing the equation (2) the calibrations were done. Mean value of all calibrations was used as sensitivity for OROS analyzer which performed the data acquisition.

### 4.3. Fatigue testing

The testing itself took place at the mechanical test-room at the room temperature of 22°C using the hydraulic MTS 2500kN testing machine.

After the testing assembly was mounted into the testing machine, strain gauges installation was prepared. First cycle applied was intended to simulate the over-speed balancing cell test (3600 rpm). 2088 kN of a quasistatic load was applied for 15 minutes. The first plastic deformation was given time to fully develop. This first cycle does not expend a significant lifetime; however, the excessive plastic strain further influences the cyclic behavior of the material. The cycles of standard over-speed tests are not included. Then, cycles simulating in-service startup and shutdown were applied. Force controlled cycle ( $R = 0.01$ ) at an amplitude of 1450kN was applied at the frequency of 0.4 Hz. Autogenous heating that could influence the low cycle fatigue behavior was neglected. It has been estimated that the maximum temperature does not exceed 40°C.

The critical spots were observed visually continuously during cycling to observe the crack initiation and to determine the number of cycles to crack initiation. Every 250 cycles the crack inspection using the magnifying glass was performed. Every 1000-2000 (or in the case of suspected indication) the test was paused and the dye penetration test was carried out to reveal crack indications. The moment of first crack detection by any means of detection was considered to be the LCF lifetime. The testing was terminated when the first observed crack reached the length of 2-4mm.

## 5. Results

### 5.1. Strain distribution

The strain distribution (von Mises equivalent strain) predicted using FEA is depicted in figure 4 (for mirrored specimen). In order to verify the prediction 3-7 strain gauges were glued on each specimen. Their emplacement and numbering is shown in figure 6. The strain was measured from the first cycle until the failure of the strain gauge or the end of testing. The strain gauges are oriented in the direction of the blade's radial line (vertical axis of the specimen). Therefore, the radial strain is measured.

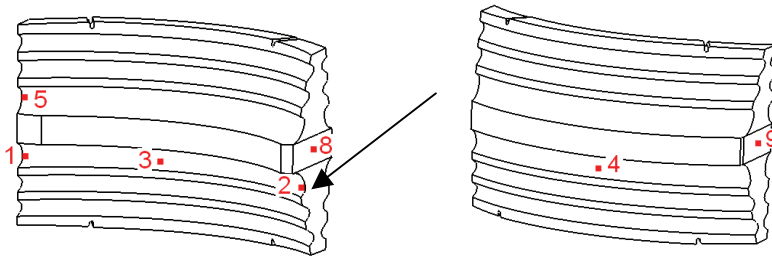


Fig. 6. Strain gauges emplacement at the testing specimen and their numbering.

Table 1 shows relative comparison of strain predicted using FEA and measured strain using strain gauges for the case of loading (in-service cycle at 1450kN). Values of strain were normalized in the way that the numerically calculated strain at the location 1 represents 100%. Other percentage values stand for the relation to this value of strain. It can be concluded that the predicted values are all within 15% tolerance compared to the measured values.

**Table 1. Relation among measured and predicted strains and strain amplitudes for all strain gauge locations for loading of 1450kN (cycle simulating in service startup and shut down)**

Number of strain gauge position	Predicted strain (FEA) for in-service cycle	Measured strain for in-service cycle	Measured strain for balancing cell over speed test type of cycle	Predicted strain amplitude for in-service cycle	Measured strain amplitude for in-service cycle
	[%]	[%]	[%]	[%]	[%]
1	100	114.2	164.8	100	100,1
2	87.8	88.3	115.3	89,1	75,6
3	36.2	40.4	54.7	49,5	51,2
4	27.4	27.9	40.7	41,0	36,8
5	54.2	62.8	92.4	64,9	62,5
8	12.7	13.7	20.0	19,4	19,9
9	17.2	20.7	31.8	26,2	29,0

Table 2 also shows the relative comparison of numerically predicted radial strain amplitude and measured strain amplitudes at the locations of strain gauges. The normalization was carried out with respect to the numerically predicted strain amplitude at the location 1. The predicted values are all within 4% tolerance compared to the measured values in the case of locations 1,3,5,8 and within 15% the case of locations 2, 4 and 9.

### 5.2. Fatigue lifetime

The fatigue crack initiated at the location indicated by arrow in figure 6; i.e. at the corner of the radius of the first groove radius – concave side; in all five cases. After crack initiation, the specimen was strained until the crack grew 2-4mm and then the

testing was terminated. The testing assembly was disassembled and the whole specimen surface was investigated employing NDT defectoscopy (Phase Array, MG) if any subsequent crack occur. No additional cracks were revealed. Therefore, the primarily detected crack is the first crack initiated. The fatigue crack initiates at the location of the second highest strain amplitude (both calculated and measured). This can be explained by the influence of the first cycle which was not investigated in this research.

The mean value of experimentally determined lifetime is the 3.6 multiple of the numerically predicted lifetime. However, the standard deviation of the measurement is relatively high – 1.76 multiple of the predicted lifetime. The experimental lifetime is probably higher due to the fact that the influence of the strain gradient and the influence of the first overloading cycle were not covered up in the numerical prediction. According to [1] the overloading cycle can improve the lifetime up to double. The influence of the strain gradient is unknown.

## 6. Conclusions

The current research has attempted to investigate the low cycle fatigue behavior of the low pressure steam turbine blade. The blade straining has been investigated using FEA. The lifetime has been predicted employing LPSA method in conjunction with uniaxial fatigue criteria. To verify the FEA analysis and lifetime prediction the testing assembly of the blade's fir tree root has been designed. The root is the critical part of the blade in terms of low cycle fatigue.

The correctness of the FEA simulation has been verified employing the strain gauge measurement. It has been concluded that the measured values correspond to the calculated ones. The lifetime prediction has been validated by straining the specimen until the occurrence of the first fatigue crack. It has been found that the predicted lifetime is lower than the experimental one. The probable reason is the influence of the strain gradient and the first overloading cycle. These influences are not incorporated in the numerical prediction. However, the predicted lifetime is not far from the scatter band of the experimental results (on the conservative side). The influence on the strain gradient which is unknown will be the matter of further investigation.

## References

- [1] Měšťánek P., *Určení životnosti závěsů turbinových lopatek parních turbin*. Thesis, (University of West Bohemia, Plzeň, Czech Republic, 2008).
- [2] Měšťánek P., "Low cycle fatigue analysis of a last stage steam turbine blade," *Applied and Computational Mechanics*, 2(1), pp. 71-82 (2008). ISSN 1802-680X.
- [3] Endo T., Kondo Y. and Kadoya Y., "Establishment of Fatigue Test Method for Turbine Blade Fastener," in *Structural Integrity of Fasteners, ASTM STP 1236*, Toor P.M., ed., (American Society for Testing and Materials, Philadelphia, 1995), pp. 20-31. ISBN 0-8031-2017-6
- [4] Klement J., Plánička F. and Vlk M., *Modelová pododnost, elektrická odporová tenzometrie, experimentální určování zbytkových napětí, vyhodnocování experimentálně získaných dat* (FAV ZČU, Plzeň, 2004).